

# SIMULATION OF THE C-BAND TRANSVERSE DEFLECTION STRUCTURE WITH VARIABLE POLARIZATION FOR SUPER TAU CHARM FACILITY\*

Sun Li, Huang Zhicheng, Cao ZeXin, Wei Yelong<sup>†</sup>

National Synchrotron Radiation Laboratory,

University of Science and Technology of China, Hefei, China

## Abstract

Transverse deflection structures (TDS) have been widely used as diagnostic devices to characterize longitudinal properties of electron bunches in a linear accelerator. However, the conventional TDS can only measure either the horizontal or the vertical slice envelopes of electron bunches. In order to give full control of the angles of the transverse streaking field inside of the TDS to characterize the projections of the beam distribution on different transverse axes, we numerically investigate a C-band TDS with variable polarization in this paper. Through variable streaking direction, the orientation of the streaking field of the TDS is adjusted to an arbitrary azimuthal angle. This helps facilitate the development of next-generation TDS for the characterization of electron bunches, such as slice emittance measurement on different planes. Here displays the simulation results of a C-band transverse deflection structure with variable polarization for preliminary study of Super Tau Charm Facility.

## INTRODUCTION

In recent years, DESY, PSI, and CERN have collaborated to develop and construct an advanced modular X-band transverse deflection structure (TDS) system[1], which has a new function of providing variable polarization of the deflection force. This innovative design has important applications in longitudinal diagnostics, e-bunch characterization, such as measurement of the energy spread, slice emittance measurements on different planes, 3D reconstruction of the charge distribution, cross correlations between the different phase spaces[2–7].

In this paper, we simulate a C-band transverse deflection structure (TDS) system, which is shown in Fig. 1. The rectangular waveguide ports transfer rf power from a rf power source (like klystron), and then through the E-rotator's mode conversion, the circular waveguide can provide required polarized mode for TDS.

## MODEL SIMULATION AND OPTIMIZATION

### E-rotator

The E-rotator is used as a mode converter, transforming the modes of two rectangular waveguides (port 1, 2) into

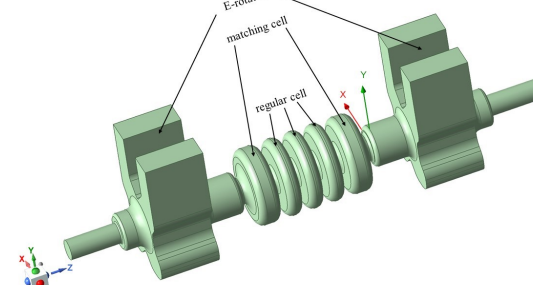


Figure 1: Schematic diagram of the TDS system with variable polarization.

circular waveguide modes (port 3). One of the input port can be configured with a variable rf phase shifter as a device to control the phase difference between two rf inputs of the E-rotator. Varying the rf phase difference from  $0^\circ$  to  $180^\circ$ , the polarization angle can be changed from horizontal to vertical continuously. The E-rotator geometry and electric field distribution for modal network result is shown in Fig. 2. Unlike traditional deflection cavities, it can provide deflection forces not only in the transverse X or Y directions.

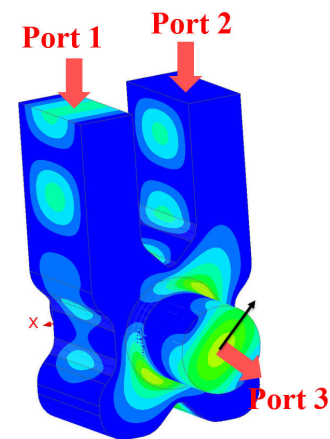


Figure 2: The E-rotator geometry and electric field distribution for modal network result. Here, the phase difference is set to 90 deg.

Here,  $FXM$  parameter is usually used to define conversion goal function in the design of E-rotator. It can be described

\* Work supported by the “Hundred Talents Program” of the Chinese Academy of Sciences, the Fundamental Research Funds for the Central Universities and Hefei Advanced Light Facility Project.

<sup>†</sup> wylong@ustc.edu.cn

by the following Equation. 1,

$$FXM = dB(0.5 - |\operatorname{Re}(S_{13x})\operatorname{Im}(S_{13y}) + \operatorname{Im}(S_{13x})\operatorname{Re}(S_{13y})|) \quad (1)$$

which  $S_{13x}$  and  $S_{13y}$  are two degenerate modes in port 3.

The simulation results of E-rotator's reflection coefficients and FXM parameter are shown in Fig. 3. The reflection coefficients  $S_{11}$  and  $S_{21}$  are -83.57 dB and -72.27 dB, respectively, and the FXM parameter is -142.48 dB.

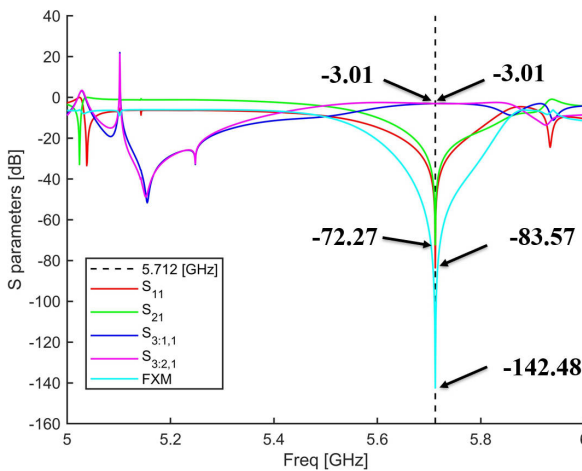


Figure 3: The reflection coefficients and FXM parameter of E-rotator.

### Regular Cell

The regular cell used as a TDS is a common constant impedance circular disk-loaded waveguide structure, which operates at  $\text{TM}_{110}$ -like mode in the backward travelling wave regime. The structure is an azimuthally symmetric cell to allow degeneracy of the two polarizations of the operating mode. Here we design a C-band TDS, which works at the rf frequency of 5.712 GHz. The geometry parameters of regular cell are given in Table 1 and shown in Fig. 4.

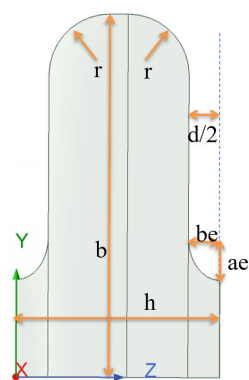


Figure 4: Cell geometry and parameter definition.

The following design parameters were used to optimize the single-cell model. The cell length  $h$  is related to the

Table 1: Geometry Parameters of the Regular Cell

Parameter	Symbol	Value
cell length	$h$	17.507 mm
cell radius	$b$	31.382 mm
rounding radius	$r$	5 mm
iris radius	$a$	8 mm
iris thickness	$d$	5.2 mm
gap	$s$	0.01
eccentricity	$e$	1.38
major axis	$ae$	$be^*$
minor axis	$be$	$d/2*(1-s)$

operating frequency and the rf phase advanced per cell  $\Delta\phi$ . The cell radius  $b$  is used to tune the eigenfrequency of the cell  $f_0$  to the operating mode frequency. The rounding radius  $r$  is maximized to increase the quality factor  $Q$  of the cell. The eccentricity  $e$  of the elliptical iris is optimized to minimize the surface fields on the iris.

The simulation results are shown in Table 2. The  $G_t$  is the transverse deflecting gradient. The  $E_s/G_t$  and  $H_s/G_t$  is the ratio of the peak surface electromagnetic field to the transverse deflecting gradient. It is essential to minimize these values in order to maximize the achievable deflection gradient. In the simulation design process, special attention was taken to minimize the Poynting vector  $S_c$ , which gives the high gradient performance limit of accelerating structures in the presence of vacuum rf breakdown[8]. The  $v_g$  is the group velocity, which is negative in the backward travelling wave structure. The  $R_t$  is the transverse shunt impedance per meter length, which represents the ability of the deflection cavity voltage that can be established under unit power loss.

Table 2: Simulation Result of the Single Cell Performance

Parameter	Symbol	Value
operating frequency	$f_0$	5.712 GHz
phase advance per cell	$\Delta\phi$	120 deg
group speed	$v_g/c$	-2.47%
quality factor	$Q$	9610
transverse shunt impedance	$R_t$	19.81 M $\Omega$ /m
normalized electric field	$E_s/G_t$	2.957
normalized magnetic field	$H_s/G_t$	12.047 mA/V
normalized Poynting vector	$S_c/G_t^2$	1.825 mA/V

The resulting distribution of the surface electric  $E_s/G_t$ , magnetic field  $H_s/G_t$  and the normalized Poynting vector  $S_c/G_t^2$  on the cell surface is shown in Fig. 5 (a, b, c), respectively.

### Matching Cell

The matching cell is used to couple the E-rotator's rf power into the regular cell with no reflections. An E-rotator and matching cell are also added at the TDS's tail for out-

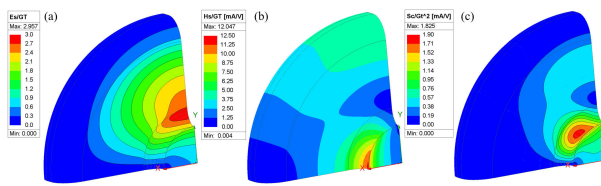


Figure 5: Distributions of the normalized electric (a) and magnetic (b) fields and of the normalized modified Poynting vector (c) on the cell surface.

putting the leftover rf power. The geometry of matching cell and three regular cell is shown in Fig. 6.

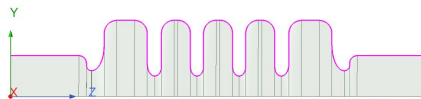


Figure 6: The geometry of matching cell and three regular cell. The red line is the surface polyline.

The shape between the matching cell and regular cell is similar, but the sizes and function are rather different. The matching cell's radius and its iris radius are used as matching parameters. By optimizing these two parameters, the reflection between matching cell and regular cell can be minimized.

Distribution of the Sc, E and H fields along the polyline are shown in Fig. 7 for Pin = 4 W.

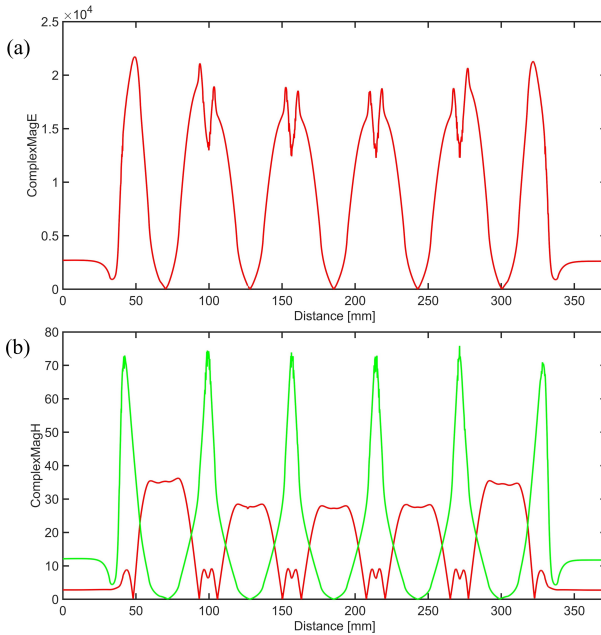


Figure 7: Distributions of the complexmagE (a) and complexmagH (b) fields along the polyline.

The matching cell's length and the iris shape is used to minimize the electric and magnetic surface fields in the

matching cell, which need to be lower than in the first regular cell. Here, complexmagE field is overall low than in the regular cells.

## CONCLUSION

This paper displays the simulation result of a C-band transverse deflection structure with variable polarization for preliminary study of Super Tau Charm Facility based on the development of Polarizable X-band TDS (PolariX-TDS) at CERN. The simulation parameters we designed have been preliminary optimized to fulfil the assumed diagnostics requirements.

## ACKNOWLEDGEMENTS

This work is supported by the “Hundred Talents Program” of the Chinese Academy of Sciences and by the Fundamental Research Funds for the Central Universities. The authors would like to thank the Hefei Comprehensive National Science Center for their strong support on the STCF key technology research project.

## REFERENCES

- [1] P. Craievich *et al.*, “Novel X-band transverse deflection structure with variable polarization,” *Phys. Rev. Accel. Beams*, vol. 23, p. 112001, 11 2020. doi:10.1103/PhysRevAccelBeams.23.112001
- [2] P. Craievich *et al.*, “Status of the polarix-tds project,” 2018. <https://api.semanticscholar.org/CorpusID:133452196>
- [3] J. Shi, A. Grudiev, and W. Wuensch, “Tuning of x-band traveling-wave accelerating structures,” *Nuclear Instruments & Methods in Physics Research Section A-accelerators Spectrometers Detectors and Associated Equipment*, vol. 704, pp. 14–18, 2013. <https://api.semanticscholar.org/CorpusID:121184957>
- [4] B. Marchetti *et al.*, “X-Band TDS Project,” in *Proc. IPAC’17*, Copenhagen, Denmark, May 2017, pp. 184–187. doi:10.18429/JACoW-IPAC2017-MOPAB044
- [5] I. Ben-Zvi, J. Qiu, and X. Wang, “Picosecond-Resolution ‘Slice’ Emittance Measurement of Electron Bunches,” in *Proc. PAC’97*, Vancouver, Canada, May 1997, pp. 1971–1975.
- [6] P. Krejcik, R. Akre, L. Bentson, and P. Emma, “A Transverse RF Deflecting Structure for Bunch Length and Phase Space Diagnostics,” in *Proc. PAC’01*, Chicago, IL, USA, Jun. 2001, pp. 2353–2355. <https://jacow.org/p01/papers/WPAH116.pdf>
- [7] P. Craievich *et al.*, “The PolariX-TDS Project: Bead-Pull Measurements and High-Power Test on the Prototype,” in *Proc. FEL’19*, Hamburg, Germany, Aug. 2019, pp. 396–399. doi:10.18429/JACoW-FEL2019-WEP036
- [8] A. Grudiev, S. Calatroni, and W. Wuensch, “New local field quantity describing the high gradient limit of accelerating structures,” *Phys. Rev. ST Accel. Beams*, vol. 12, p. 102001, 10 2009. doi:10.1103/PhysRevSTAB.12.102001